Electrochemical sensing of Pb(II) and Cd(II) in decorative material of wood panel using nano-cellulose paper-based electrode modified using Graphene/Multi-walled Carbon Nanotubes/Bismuth film

Hui Wang[1], Junfeng Wang [3], Gang Liu[2], Zhankuan Zhang[1], and Xiaopeng Hou[1]*

[1] Research Institute of Wood Industry, Chinese Academy of Forestry, Beijing 100091, China;
[2] Key Laboratory of Modern Precision Agriculture System Integration Research, Ministry of Education and Key Laboratory of Agricultural Information Acquisition Technology, Ministry of Agriculture, China Agricultural University, Beijing 100083, China
[3] Guanxi Zhuang Autonomous Region Forestry Research Institute, Nanning 530002, China
*E-mail: hello168429@sina.com and wanghui_lunwen@163.com

The yield of decorative material of wood panel is unceasingly rising with the increasing output of the wood panel. Parts of decorative materials contains soluble heavy metals, which will probably pollute the environment. To monitor the contaminations of Cd(II) and Pb(II), nanocellulose paper was used as the substrate, a room temperature ionic liquid was applied as a conductive binder to improve the conductivity, and a nanocomposite of graphene/multi-walled carbon nanotubes (G-MWNTs) was modified the electrode' surface to increase the specific surface area. The characteristics of the paper-based electrode (PBE) before and after functionalized with G-MWNTs were investigated by scanning electron microscopy, cyclic voltammetry, and electrochemical impedance spectroscopy. Moreover, bismuth film was electroplated on the G-MWNTs/PBE in-situ to improve the sensitivity for Cd(II) and Pb(II). The current responses of Cd(II) and Pb(II) were activated on Bi/G-MWNTs/PEB using square wave stripping voltammetry. Under the optimized paramters, the current responses of Cd(II) and Pb(II) were positive linear relation with a wide concentration range from 1 μg/L to 50 μg/L with the limits of detection were 0.2 μg/L (S/N=3). Finally, the Bi/G-MWNTs/PBE was successfully used as a useful probe to determine the Cd(II) and Pb(II) in decorative material of wood-based panel with good results.

1. INTRODUCTION

Wood panels are manufactured into furniture, floors, cabinets, doors and windows, which play an essential role in people's living and working environment [1, 2]. The yield of decorative material of

wood panel is unceasingly rising with the increasing output of the wood panel. These decorative materials [3, 4, 5] include impregnated paper, decorative wood-grain paper, PVC film, and paint, which are often added additives such as colorants, flame retardants, stabilizers and fungicides to improve or increase the aesthetic, durability and stability. However, parts of dyes, fungicides, and flame retardants contain heavy metal compounds that might pollute the indoor environment [6]. In addition, the waste of decorative material also can cause heavy metal pollution in the outdoor environment [7].

Soluble heavy metal contamination [8] includes lead, cadmium, chromium, mercury, and other pollution sources. These heavy metals existed in the exterior and interior environment is likely to enter the human body through the food chain or skin contact [9], especially children's hands. Heavy metal ions can bind with the active groups of protein molecules in animal or human, changing the structure or charge of protein molecules that deprive their biological functions. Some heavy metal ions have similar properties to the essential metal ions that can replace the critical metal ions to occupy the coordination site, which will interfere with the metabolism of the essential metal ions and produce high toxicity to organisms. Their long-term contact with skin can cause contact dermatitis or eczema, which is harmful to human nervous and visceral systems, especially to children's development.

To ensure human health, limitation standards for heavy metals in decorative materials have been established in developed countries, which have exploited many detection techniques. The corresponding standards in China also been established, such as "Determination of soluble heavy metals in paints and varnishes (GB/T 9758)", "Limitation of harmful substances in Solvent-based wood coatings (GB 18581)" and "Limitation of harmful substances in interior wall coatings (GB 18582)". To monitor the concentrations of Cd(II) and Pb(II), a cheap and convenient analytical tool is urgent to develop for the determination of heavy metal ions. Presently, heavy metals were mainly measured by the spectral analysis methods, including atomic absorption spectrometry (AAS) [10], inductively coupled plasma emission spectrometry (ICP-AES) [11], X-ray fluorescence spectrometry (X-ray) [12], inductively coupled plasma mass spectrometry (ICP-MS) [13] and atomic fluorescence spectrometry (AFS) [14] and ultraviolet-visible spectrophotometer (UV-vis) [15]. These methods have been applied in the hazardous substance analysis institutions with high accuracy, but analytical instruments are bulky, expensive, and complex to operate [16]. The electrochemical electrode is a new method that is widely used in different fields owing to its low cost, ease of use, and cheap device [17].

Screen-printed electrode (SPE) are fabricated through screen printing techniques, which is currently extensively researched in analyzing measuring domain with essential advantages in terms of sensitivity, accuracy, reliability and low cost [18, 19]. The SPE consists of three parts: substrate, ink, and modifier. The typical substance [20, 21] includes paper, polymer films, plastics, ceramics, and even flexible and elastic clothing materials to meet different demands of using. Inexpensive and conductive carbon materials are often used as ink materials in SPEs with low sensitivity and poor selectivity, which is hard to trace the super-low level of Cd(II) and Pb(II). Thus, versatile modifiers including metals, enzymes, functional carbon materials, polymers, and complexing agents are employed to improve the sensitivity and selectivity. Paper-based electrodes (PBD) [22, 23] have attracted widespread attention because of their inherent advantages in many applications. PBD with different modifiers can provide simplicity, portability, reproducibility, low-cost, high selectivity, and sensitivity for analytical measurements in a variety of applications [24]. Ionic liquid, n-octyl pyridinium hexafluorophosphate

(OPFP), is a conductive, non-volatile, and non-combustible material in comparison with other electrolyte aqueous solutions [25, 26]. OPFP has been applied to fabricate or modify the electrodes with excellecent electrochemical behavior, which increases remarkablily the electron transfer rate among different electroactive compounds and decreases the hydrogen-cherged potential. An electrochemical carbon electrode was fabricated using OPFP as binder and palladium nanoparticles as a modifier to evaluate the isoniazid in human blood serum and pharmaceutical samples [27]. Due to its excellent optical, electrical and mechanical properties, graphene [28] as a monolayer of graphite has become applied in material science, energy, analytical chemistry, biomedicine, and drug delivery. There are many methods to produce graphene [29], but the chemical reduction is expected to the mass production because of its low cost, high efficiency, and facile functionalization. Multi-walled carbon nanotubes [30] has unique mechanical, geometric, electronic, and chemical properties that are progressively paid attention in electrochemical detection.

In the current study, a sensitive and selective electrode with low-price was explored to monitor the levels of Cd(II) and Pb(II). Nanocellulose paper was used as the substrate, a room temperature ionic liquid was applied as a conductive binder to improve the conductivity, and a nanocomposite of graphene/multi-walled carbon nanotubes (G-MWNTs) was modified the electrode' surface to increase the specific surface area. Moreover, bismuth film was electroplated on the G-MWNTs/PBE in-situ to improve the sensitivity for Cd(II) and Pb(II), and the current responses of Cd(II) and Pb(II) were obtained by square wave stripping voltammetry.

2. EXPERIMENT

2.1 Chemicals and reagents

The following chemicals were purchased from Nanjing Xianfeng Nanomaterials Technology Co., Ltd and used as received: graphene oxide and multi-walled carbon nanotube. N-octyl pyridinium hexafluorophosphate and graphite powder (size<30 μm, spectral pure grade) were provided from Sinopham Chemical Reagent Co., Ltd. Cyclohexanone, acetone and dimethyl formamide obtained from Beijing Chemical Industry Group Co., LTD. Dimethylglyoxime (DMG), potassium ferricyanide ($K_3[Fe(CN)_6]$) and potassium ferrocyanide ($K_4[Fe(CN)_6]$) were purchased from National Research Center for Certified Reference Material (China). The standard solutions of Cd(II), Pb(II) and Bi(III) were obtained from Beijing Yihua Tongbiao Technology Co., LTD. All of chemicals and reagents were analytical reagent grade, which were not further purified.

Electrochemical characterization of G-MWNTs/PBE was conducted in 5 mmol/L $K_4[Fe(CN)_6]$ and $K_3[Fe(CN)_6]$, and the supporting electrolyte was 0.1 mol/L acetate buffer for the Cd(II) and Pb(II) detection. Various heavy metal concentrations of Cd(II) and Pb(II) were diluted from standard solutions. All solutions were prepared using Milli-Q purified water.

2.2 Instruments

An electrochemical workstation CHI760E purchased from Shanghai Instrument Company was applied in the electrochemical analysis. The Bi/G-MWNTs/PEB was served as the working electrode.

Printed silver electrode and printed carbon electrode were used as reference electrode and counter electrode, respectively. A KMS-131E magnetic stirrer provided by Shanghai Jingchi Technology Co., LTD was used for stirring and a PHS-3C digital pH-meter offered by Shanghai instrument scientific instrument co., LTD was employed to adjust the pH value. All experimental measurements were performed at room temperature.

2.3. Preparation of the Electrode

The nanocellulose paper-based electrode was prepared in bulk as follows. Non-electrode structure area on the ordinary paper was printed using PDMS. The nanocellulose solution was directly dripped onto the electrode structure area to form a uniform nanocellulose film. An organic solvent was prepared by mixing 5 mL cyclohexanone and 5 mL acetone, which added and dissolved 0.1 g cellulose acetate, 1 g OPFP, and 4 g graphite powder, respectively. The mixed ink was printed on the area of the working electrode and the counter electrode, and the reference electrode was made of silver-silver chloride. The nanocellulose paper-based electrode (PBE) was dried at 50 ℃.

Multi-wall carbon nanotubes modified by carboxylic groups (c-MWNTs) were evenly dispersed in ultra-pure water by ultrasonic treatment, and graphene oxide (G) were added and dissolved into ultra-pure water, respectively. Then the same volumes of these two solutions were mixed to form a uniform solution (G-MWNTs) by ultrasonic dispersion for 30 minutes. The dispersed solution of G-MWNTs was dropped on PBE and then was dried in ambient air at 60 °C. Finally, G-MWNTs/PBE was immersed in 0.1 mol/L PBS (pH 7.0) and reduced the graphene oxide through cyclic voltammetry with scan rate 20 mV/s.

2.4 Measurement Procedures

Electrochemical measurements using the prepared electrodes were performed in a 0.1 mol/L acetate buffer solution at room temperature. The G-MWNTs/PBE was firstly operated below -1.3 V for 300 s with stirring conditions. The parameters of the square wave anodic stripping voltammetry (SWASV) were 10 s equilibration period, 25 mV square wave amplitude, 5 mV potential step, and 25 Hz frequency.

2.5. Analysis of Real Samples

For the paint on the surface of the floor, (a) scraping appropriate amount of the paint from the surface with a scraper; (b) crushing at room temperature through a magnetic stirrer; (c) sieving the ground using 0 .5 mm sifter; (d) weighing 0 .2 paint mixed with g placed 10 mL of a hydrochloric acid solution; (e) the mixture was sonicated at 37 °C for 1 h; (f) the supernatant was filtered, and then adjusted the pH.

3. RESULTS AND DISCUSSION

3.1 Characterization

The images of SEM were used to characterize the morphology of PBE before and after modified reduced graphene oxide and multi-walled carbon nanotubes. Fig. 1(a) shows the structure of the PBE displayed some large uplift and the uneven surface. When the PBE was modified with G-MWNTs, the typical wrinkled character with the high-density tubular structure were distributed on the surface, which was similar to the microstructure of the graphene and multi-walled carbon nanotubes [31]. It confirmed that the reduced graphene oxide and multi-walled carbon nanotubes had been dispersed in the Milli-Q purified water homogeneously and coated on the PBE' surface uniformly, which can increase the effective contact area between G-MWNTs/PBE and heavy metal ions.
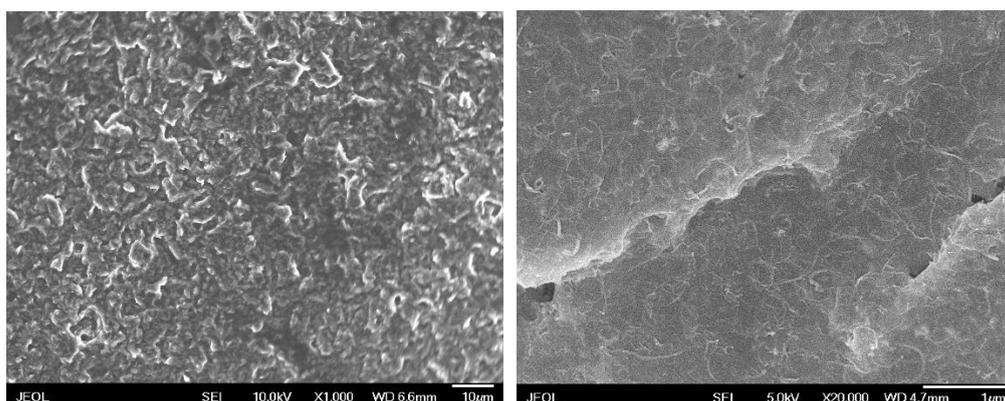
Figure 1. SEM images of PBE(a) and G-MWNT/PBE (b).

Cyclic voltammetry (CV) was used to investigate the electrochemical behavior of commercial SPE, PBE and G-MWNT/PBE with a scan rate of 50 mV/s in 5 mmol/L $[Fe(CN)_6]^{3-/4-}$ containing 0.1 mol/L KCl. As shown in Fig. 3, the current redox responses of the commercial SPE was about 70 μA with the peak-to-peak separation of 320 mV. For the PBE, the current redox response was about 85 μA higher and the peak-to-peak separation decreased to 120 mV, the redox peak potentials were lower than those at the commercial SPE, which was attributed to the electrochemically active sites of the ink added ionic liquid that can improve the charge transfer. Moreover, the current redox responses at the G-MWNTs composite modified PBE were significantly higher than SPE and PEB. The main reason was the large specific surface area and fast electron transfer rate of the nano-composite membrane of G-MWNTs [32].
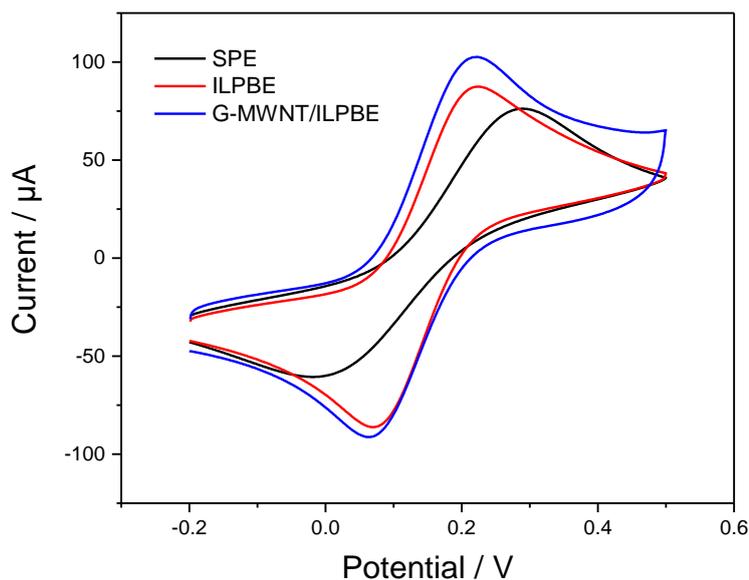
Figure 2. CV curves of commercial SPE, PBE, and G-MWNT/PBE in 5 mmol/L $[Fe(CN)_6]^{3-/4-}$ containing 0.1 mol/L KCl with the scan rate: 50 mV/s during the potential between -0.2 and 0.5 V.

EIS was an effective electrochemical method to describe the impedance changes of different electrodes modified different materials. The EIS curve was consisted by two parts: a linear region at the lower frequencies and a semicircle region at higher frequencies, which represented the diffusion process and the electron transfer resistance (R_{et}), respectively.
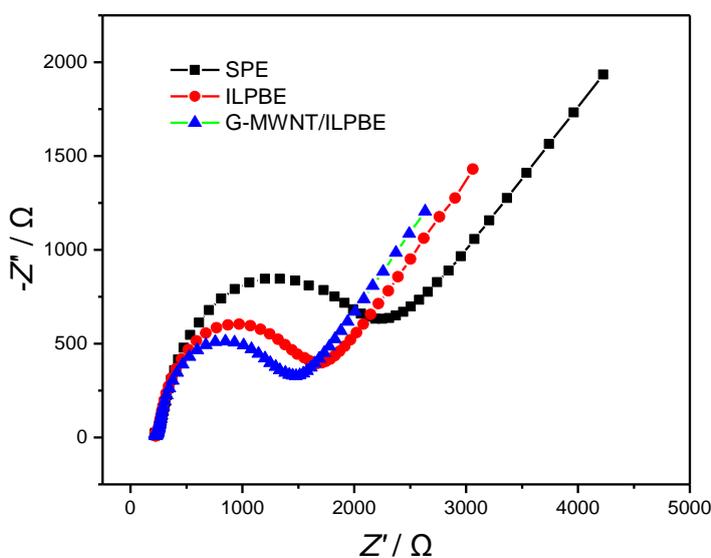
Figure 3. Electrochemical impedance spectra of commercial SPE, PBE and G-MWNT/PBE with the frequencies from 1 to 10^5 Hz in 5 mmol/L $[Fe(CN)_6]^{3-/4-}$ and 0.1 mol/L KCl

As shown in Figure 3, the R_{et} value of commercial SPE was about 2 kΩ. After G-MWNTs was immobilized on PBE, the impedance between G-MWNTs and electrolyte was decreased, and the R_{et} value decreased to 800 Ω, which was ascribed to the synergistic effect of G-MWNTs. Similarly, R_{et} value of the RGO-MWNT/SPE was about 1100 Ω The results were in agreement with the conclusion obtained from the CV.

The potential windows of G-MWNTs/PBE and Bi/G-MWNTs/PBE were measured using cyclic voltammetry with the scan rate of 100 mV/s in Figure 4. The negative potential window of G-MWNTs/PBE was about -1.1 V, which was closed to the stripping potential of Cd(II). After G-MWNTs/PBE electroplated a Bi film, it was clear that the negative potential window of Bi/G-MWNTs/PBE reached -1.4 V, which was contributed to the special crystal plane structure of bismuth that decreased the hydrogen evolution potential of G-MWNTs/PBE [33].
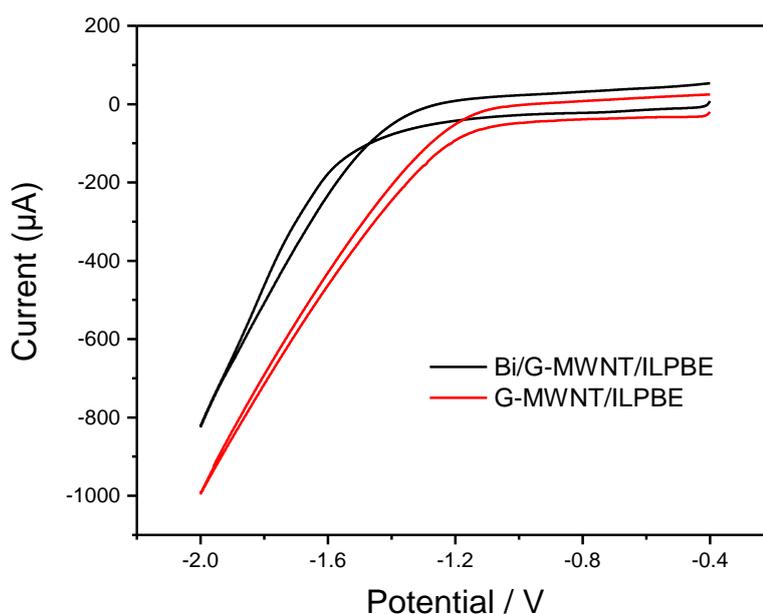
Figure 4. Cyclic voltammograms of G-MWNTs/PBE and Bi/G-MWNTs/PBE in 0.1 mol/L acetate buffer solution with the scan rate 100 mV/s

Figure 5 shows the SWV responses of G-MWNTs/PBE and Bi/G-MWNTs/PBE, which were used to measure 40 µg/L Cd(II) and 40 µg/L Pb(II). The stripping currents for Cd(II) and Pb(II) located at -1.0 V and -0.8 V because Ag electrode was insteaded by Ag/AgCl electrode, which the electrode potential of Ag electrode was higher than the Ag/AgCl electrode. The current responses of Bi/G-MWNTs/PBE were much higher than G-MWNTs/PBE, which was ascribed to bismuth can bind with cadimium and lead to form alloy [34].
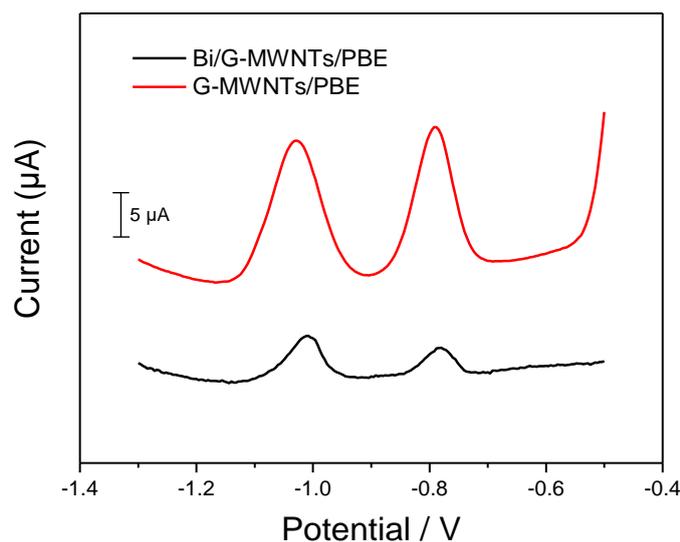
Figure 5. The SWV responses of G-MWNTs/PBE before and after electroplated Bi film in 40 µg/L Cd(II) and 40 µg/L Pb(II)

3.4 Optimization of experimental conditions

To optimize the detecting parameters, the Bi/G-MWNT/PDE was used to measure the 40 µg/L Cd(II) and 40 µg/L Pb(II) using SWV measurement in the 0.1 mol/L sodium acetate buffer solution.

The pH of the supporting electrolyte has a noteworthy influence for the current response of Cd(II) and Pb(II). Figure 6(a) shows the current responses changed with the pH in the range from 3.5 to 5.5. When the pH was lower than 4.5, the current responses were positively correlated with the pH of the supporting electrolyte. The reason was that H(I) might be reduced to hydrogen on the Bi/G-MWNTs/PBE's surface that will damage the bismuth film. On the contrary, the current responses decreased at higher pH 4.5, which was ascribed to the formation of metal hydroxide complexes at higher pH. Thus, the pH of the supporting electrolyte optimum was determined to be 4.5.

Figure 6(b) shows the current responses of Cd(II) and Pb(II) affected by the Bi(III) concentrations in the range from 0 to 3.0 mg/L. The current responses of Cd(II) and Pb(II) were significantly correlated with the thickness of bismuth. The current responses enhanced gradually with increasing the Bi(III) concentration from 0 to 2 mg/L because Bi(III) can form a complex with Cd(II) and Pb(II) that reduced them easily. However, the current responses of Cd(II) and Pb(II) decreased after the Bi(III) concentration exceeded 2 mg/L, indicating that a thick bismuth film might hinder the mass transfer of Cd(II) and Pb(II). Therefore, 2 mg/L of Bi(III) concentration was selected in the experiments.
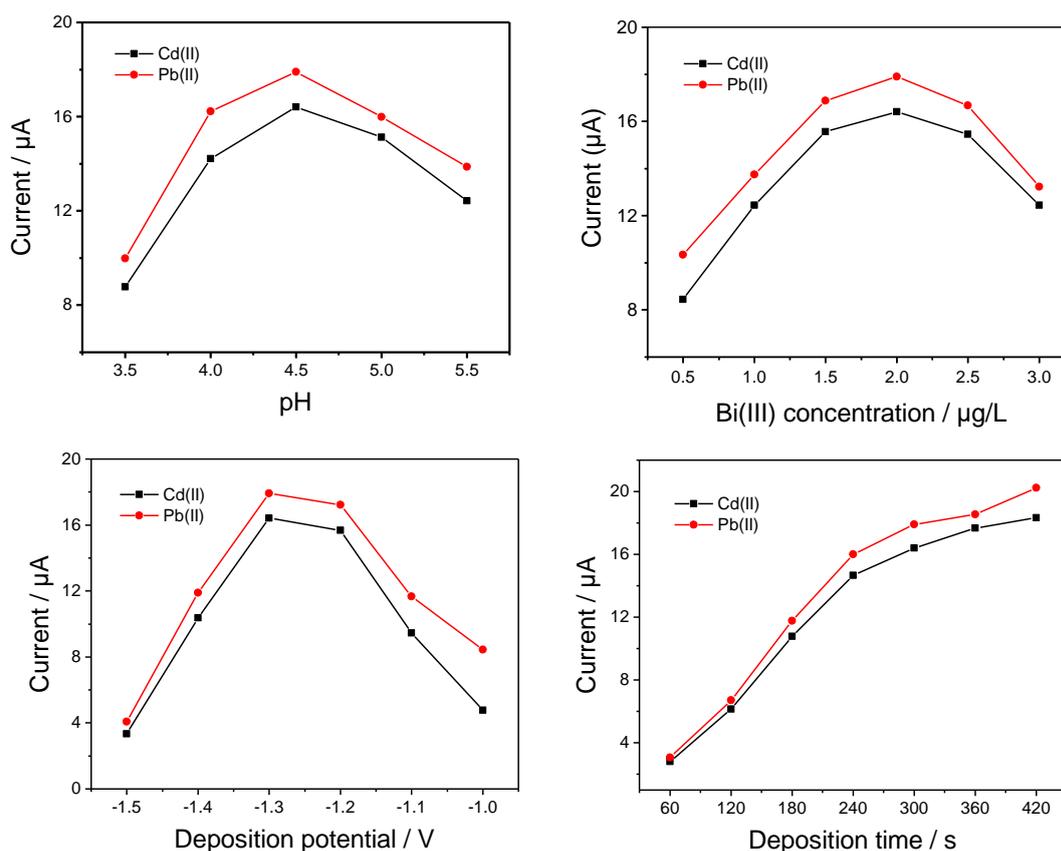
Figure 6. The current responses for the determination of 40 μg/L Cd(II) and 40 μg/L Pb(II) in 0.1 mol/L acetate buffer solution affected by (a) bismuth concentration, (b) pH value, (c) deposition potential and (d) deposition time

The deposition potential is a significant factor to enhance the sensitivity of Bi/G-MWNTs/PBE. Figure 6(c) shows that the current responses for Cd(II) and Pb(II) were changing with the deposition potential ranging from -1.5 V to -1.0 V. The current responses exhibited a notable increasing trend with positive shifts of the deposition potential, which reached the maximum at -1.3 V. When the accumulation potential was more negative than -1.3 V, the current responses reduced. The reason was that the hydrogen interfering with the determination was produced at more negative potentials that might damage the metal alloy deposition at the electrode surface [35]. Thus, the deposition potential of -1.3 V was chosen as the optimum value for Cd(II) and Pb(II).

The deposition time can help to improve the sensitivity of Bi/G-MWNTs/PBE. Figure 6(d) shows the current responses of Cd(II) and Pb(II) were affected by the deposition time. The current responses of Cd(II) and Pb(II) were growing with prolonged deposition time. However, the slope of the curved plot began to diminish if the deposition time was longer than 300 s. Only a slight increase of the currents response was found because the amount of Cd(II) and Pb(II) was saturated on the electrode surface. Thus, 300 s was selected as the optimum deposition time.

3.4 Analytical performance

Based on the optimized parameters mentioned above, pH 4.5, 2 mg/L of Bi(III) concentration, a deposition potential of -1.3 V and a deposition time of 5 min were selected to investigate the linear rang of the Bi/G-MWNTs/PBE for the Cd(II) and Pb(II). Figure 7 shows the SWV responses of the Bi/G-MWNTs/PBE exposed to different concentrations of Cd(II) and Pb(II). It was clear that the current responses were increasing with the increasing concentrations of Cd(II) and Pb(II), which exhibited a linear relationship. The two insets revealed that the curent responses were linear with the concentration of Cd(II) and Pb(II) over the range of $1 \sim 50$ µg/L. The regression equations were: $I(\mu A)=0.4065 \times C(\mu g/L) +0.5235$ and $I(\mu A)=0.4437 \times C(\mu g/L)+10655$ with the correlation coefficients of 0.99 and 0.99, respectively. The limits of detection were 0.2 µg/L and 0.2 µg/L for Cd(II) and Pb(II) based on three times the standard deviation of the baseline (S/N=3).
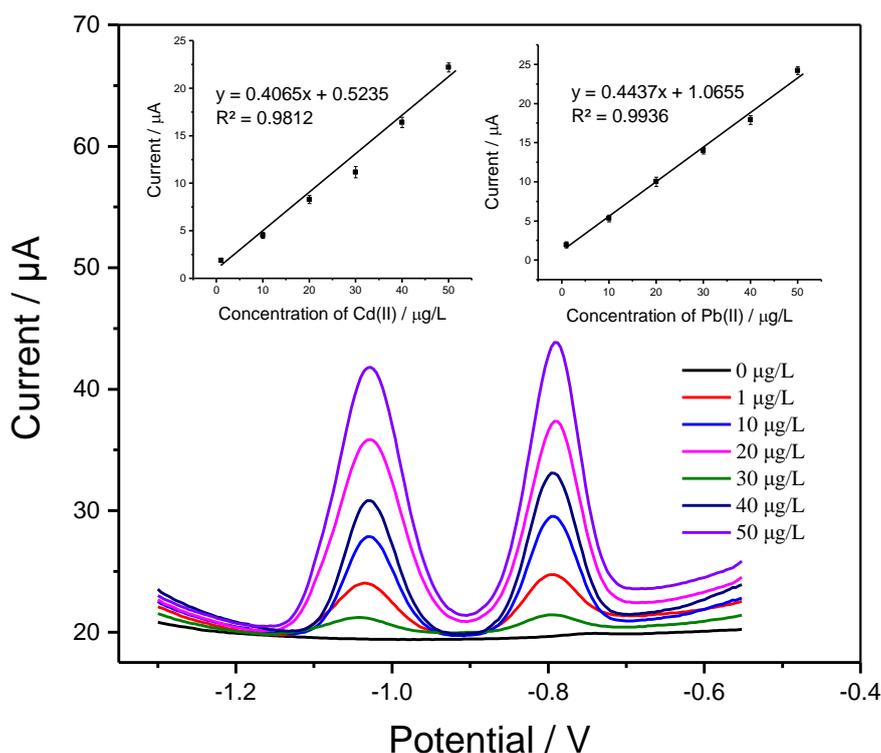
Figure 7. SWASV curves of the Bi/G-MWNTs/PBE to detect different Cd(II) and Pb(II) concentrations ranging from 1 *µ*g/L to 50 *µ*g/L; (A) The calibration curve of Cd(II); (B) The calibration curve of Pb(II)

The detecting parameters of the electrochemical electrodes reported previously were listed in Table 1. In comparesion with these electrodes, the proposed electrode for the Cd(II) and Pb(II) detection exhibited excellent detecting performance, which had wider linear range and lower limit of detection. The detection time was much longer than most electrodes, but it can satisfy the requirementsin routine analysis .

Table 1. Comparison of the performance parameters of different electrodes for the Cd(II) and Pb(II) detection

Electrodes	Liner rang (μg/L)		Limit of detection (μg/L)		Detection time (s)	References
	Cd(II)	Pb(II)	Cd(II)	Pb(II)		
Nafion/Bi/NMC/GCE	2~100	0.5~100	1.5	0.05	150	[36]
Bi/SPE	0.5~12	0.5~12	0.2	0.2	120	[37]
BiFE/GCE	5~60	5~60	0.4	0.8	600	[38]
ZnO@G/SPCE	10~200	10~200	0.6	0.8	180	[39]
Bi₂O₃/PSS/CnP/SPCE	5~40	5~40	0.1	0.3	420	[40]
ERGNO film/SPCE	1~60	1~60	0.5	0.8	150	[41]
BiF/SWNHs/SPE	1~60	1~60	0.2	0.4	150	[42]
GR/L-cys/Bi/SPE	10~50	10~50	0.98	0.56	180	[43]
SSE	31.7~317.5	15.5~1035	6.8	14.6	300	[44]
Bi/RGO-MWNT/PBE	1~50	1~50	0.2	0.2	300	This work

3.5 Interference effects

The anti-interference was an essential factor for electrochemical electrode. Bi/G-MWNT/PBE was employed to detect the standard solutions of Cd(II) and Pb(II) under the optimal conditions, which also co-existed with different metal ions including K(I), Mg(II), Ca(II), Hg(II), Zn(II), Fe(III), Al(III), Cl(I) and NO₃(I). The current responses of Cd(II) and Pb(II) were shown in Figure 8. The relative errors were lower than 5%, indicating that no significant current response change was observed in the presence of other metal ions except for Cd(II) and Pb(II). These data indicated that Bi/G-MWNTs/PBE exhibited excellent selectivity toward Cd(II) and Pb(II).
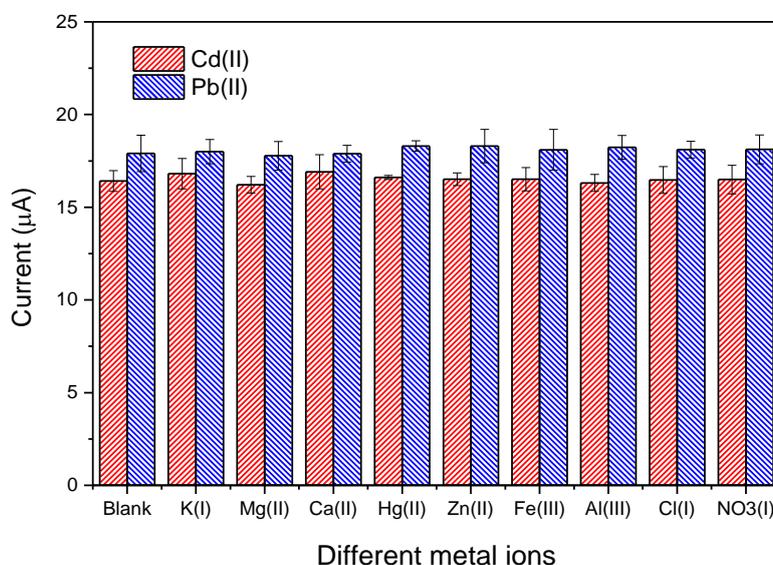
Figure 8. The selectivity of the sensing system for 40 μg/L Cd(II) and 40 μg/L Pb(II) over other competing metal ions.

3.6 Reproducibility

To study the reproducibility, five different Bi/G-MWNT/PBE were fabricated using the protocol mentioned above, and then were applied to determine the 40 μg/L Cd(II) and 40 μg/L Pb(II). Figure 9 shows the current responses of five different Bi/G-MWNT/PBE for Cd(II) and Pb(II). The relative errors were lower than 5 %, indicating that the Bi/G-MWNT/PBE had excellent reproducibility.
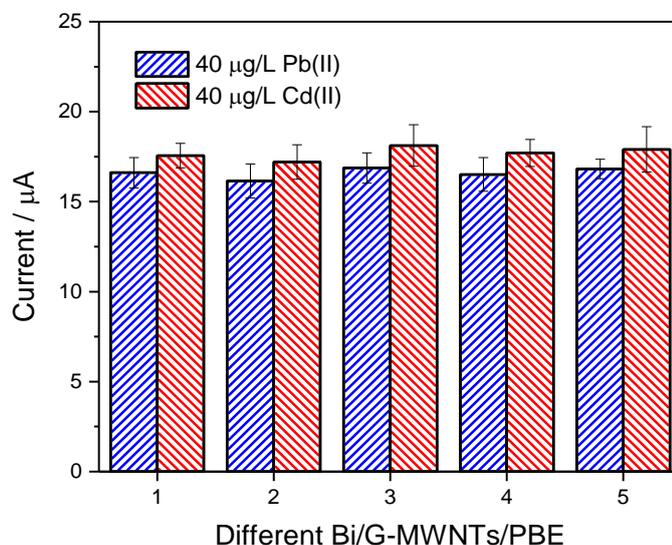
Figure 9. The current responses using five different Bi/G-MWNT/PBE for 40 μg/L Cd(II) and 40 μg/L Pb(II).

3.7 Stability

To determine the storage stability of the Bi/G-MWNT/PBE, the electrodes were stored in air at room temperature, and the sensitivity was checked every day. After five days, Bi/G-MWNT/PBE was determined the 40 μg/L Cd(II) and 40 μg/L Pb(II) that the values of current response were no obvious changes in contrast with the initial values, suggesting that Bi/G-MWNT/PBE was highly stable in air.

3.8 Analysis of the samples

To evaluate the application, Bi/G-MWNTs/PBE was applied to measure the concentrations of Cd(II) and Pb(II) in decorative material of wood panel. All the samples were collected from the wooden floor. Before measurement, the samples were pretreated to extract the soluble Cd(II) and Pb(II) in the paint through the protrocal in 2.5. The extracting solutions were detected by the Bi/G-MWNTs/PBE and flame atomic absorption spectrometry (FAAS), respectively. Then, the solutions added 10 μg/L of Cd(II) and Pb(II) were measured by Bi/G-MWNTs/PBE again. The results were shown in Table 2. It can be seen that the recoveries of Cd(II) and Pb(II) were ranging from 92.72% to 107.89%, which can meet the requirement of routine analysis .

Table 2. Results for the Cd(II) and Pb(II) detection in real samples

Sample	Add (µg/L)	Bi/G-MWNTs/PBE (µg/L)		FAAS (µg/L)		Recovery (%)	
		Cd(II)	Pb(II)	Cd(II)	Pb(II)	Cd(II)	Pb(II)
1	-	13.43±0.64	27.38±0.84	14.11	27.89	95.18	98.17
	10	23.83±0.78	38.16±1.45			98.83	100.71
2	-	9.62±0.77	19.89±1.12	9.21	18.63	104.45	106.76
	10	20.35±0.93	30.89±1.34			105.93	107.89
3	-	15.21±0.94	5.85±0.15	15.89	6.32	95.72	92.72
	10	26.78±0.83	15.75±0.87			103.43	96.51
4	-	11.32±0.87	16.11±1.10	11.56	16.76	97.92	96.12
	10	22.56±1.23	26.98±1.87			104.63	100.82

4. CONCLUSION

In this study, we had fabricated an electrochemical electrode using PBE modified GO and MWNTs and then electroplated the Bi film to the detection of Cd(II) and Pb(II) simultaneously. The limits of detection were as low as 0.2 µg/L and 0.2 µg/L toward Cd(II) and Pb(II). The Bi/G-MWNTs/PBE took advantages of the paper electrode, carbon nanomaterials, and ionic liquid, which exhibited high selectivity, reproducibility and stability. Furthermore, the electrode exhibited excellent anti-interference that could measure the levels of Cd(II) and Pb(II) in decorative materials of wood panel with good results.

References

1. M. Rebollar, R. Pérez, R. Vidal, *Mater. Design*, 28 (2007) 882.
2. A. Cobut, P. Blanchet, R. Beauregard, *Forest Prod. J.*, 66 (2016) 196.
3. A. B. Amor, A. Cloutier, R. Beauregard, *Wood Fiber Sci.*, 41 (2009) 117.
4. JozefKÃ°dela and EvaLiptÃ¡kovÃ¡, *J. Adhes. Sci. Technol.*, 20 (2006) 875.
5. J. H. Chen, F. U. Zhong-Ping, *Liaoning Chem. Ind.*, 10 (2015) 72.
6. L. Long, A. M. Huang, D. Meng, Z. G. Lu, *Spectrosc. Spect. Anal.*, 32 (2012) 2572.
7. D. Meng, L. Long, L. V. Bin, A. M. Huang, *China Wood Industry,* 3 (2012) 65.
8. X. Yang, J. Liu, K. McGrouther, H. Huang, K. Lu, X. Guo, L. He, X. Lin, L. Che, Z. Ye, *Environ. Sci. Pollut. R.*, 23 (2016) 974.
9. K. S. Balkhair and M. A. Ashraf, *Saudi J. Biol. Sci.*, 23 (2016) S32.

10.   Y. Koike, K. Hagiwara, T. Nakamura, *Anal. Chem. Res.*, 11 (2017) 9.
11.   N. R. Biata, L. Nyaba, J. Ramontja, N. Mketo, P. N. Nomngongo, *Food Chem.*, 237 (2017) 904.
12.   M. Qu, Y. Wang, B. Huang, Y. Zhao, *Environm. Pollut.*, 240 (2018) 184.
13.   Z. H. Wang, Z. H. Shi, J. F. Cai, Q. J. Wu, *Modern Food Sci. Tech.*, 33 (2017) 276.
14.   E. Saouter and B. Blattmann, *Anal. Chem.*, 66 (1994) 2031.
15.   Y. Guo, H. Zhao, Y. Han, X. Liu, S. Guan, Q. Zhang and X. Bian, *Spectrochimica Acta A,* 173 (2017) 532.
16.   H. Wang, Y. Liu, G. Liu, *Microchim. Acta*, 185 (2018) 142.
17.   H. Wang, Y. Liu, G. Liu, *ACS sensors,* 3 (2018) 624.
18.   W. Hui, Y. Yin, G. Zhao, F. Bienvenido, I. M. Flores-Parrad, Z. Wang, G. Liu, *Int. J. Agr. Biol. Eng.*, 12 (2019) 194.
19.   H. Wang, G. Zhao, Y. Yin, Z. Wang, G. Liu, *Sensors,* 18 (2018) 6.
20.   W. Zeng, L. Shu, Q. Li, S. Chen, F. Wang, X. M. Tao, *Adv. Mat.*, 26 (2014) 5310.
21.   J. Kim, R. Kumar, A. J. Bandodkar, J. Wang, *Adv. Electron. Mater.*, 3 (2017) 1600260.
22.   J. Mettakoonpitak, K. Boehle, S. Nantaphol, P. Teengam, J. A. Adkins, M. Srisa‐Art, C. S. Henry, *Electroanal.*, 28 (2016)1420.
23.   M. Santhiago, J. B. Wydallis, L. T. Kubota, C. S. Henry, *Anal. Chem.*, 2013, 85, 5233-5239.
24.   C. Zhu, G. Yang, H. Li, D. Du, Y. Lin, *Anal. Chem.*, 87 (2014) 230.
25.   N. Maleki, A. Safavi,F. Tajabadi, *Anal. Chem.*, 78 (2006) 3820.
26.   H. Wang, Y. Duan, G. Zhao, Z. Wang, G. Liu, *Int. J. Electrochem. Sci.*, 10 (2015) 8759.
27.   G. Absalan, M. Akhond, M. Soleimani , H. Ershadifar, *J. Electroanal.Chem.*, 761 (2016) 1.
28.   X. Li, X. Wang, L. Zhang, S. Lee, H. Dai, *Science*, 319 (2008) 1229.
29.   Y. Zhu, S. Murali, W. Cai, X. Li, J. W. Suk, J. R. Potts, R. S. Ruoff, *Adv. Mat.*, 22 (2010) 3906.
30.   G. Başkaya, Y. Yıldız, A. Savk, T. O. Okyay, S. Eriş, H. Sert, F. Şen, *Biosens. Bioelectron.*, 91 (2017) 728.
31.   P. Han, Y. Yue, Z. Liu, W. Xu, L. Zhang, H. Xu, G. Cui, *Energ. Environ. Sci.*, 4 (2011) 4710.
32.   C. Zheng, X. Zhou, H. Cao, G. Wang, Z. Liu, *J. Power Sources,* 258 (2014) 290.
33.   S. Dal Borgo, V. Jovanovski, B. Pihlar, S. B. Hocevar, *Electrochim. Acta*, 155 (2015) 196.
34.   Y. Yin, H. Wang, G. Liu, *Int. J. Electrochem. Sci.*, 13 (2018)10259.
35.   Z. Wang, H. Wang, Z. Zhang, G. Liu, *Sensor. Actuat. B-Chem*, 199 (2014)7-14.
36.   L. Xiao, H. Xu, S. Zhou, T. Song, H. Wang, S. Li, W. Gan, Q. Yuan, *Electrochim. Acta,* 143 (2014) 143.
37.   D. Riman, D. Jirovsky, J. Hrbac, M. I. Prodromidis, *Electrochem. Commun.*, 50 (2015) 20.
38.   D. Yang, L. Wang, Z. Chen, M. Megharaj, R. Naidu, *Microchim. Acta*, 181 (2014) 1199.
39.   J. Yukird, P. Kongsittikul, J. Qin, O. Chailapakul, N. Rodthongkum, *Synthetic Met.*, 245 (2018) 251.
40.   R. María-Hormigos, M. J. Gismera, J. R. Procopio, M. T. Sevilla, *J. Electroanal. Chem.*, 767 (2016) 114.
41.   J. Ping, Y. Wang, J. Wu, Y. Ying, *Food. Chem.*, 151 (2014) 65.
42.   Y. Yao, H. Wu, J. Ping, *Food Chem.*, 274(2019) 8.
43.   C. Li, X. Zhao, X. Han, *Anal. Methods-UK.*, 10 (2018) 4945.
44.   S. A. Kitte, S. Li, A. Nsabimana, W. Gao, J. Lai, Z. Liu, G. Xu,. *Talanta*, 191 (2019) 485.